



Development of an *Escherichia coli* whole cell biocatalyst for the production of hyperoside

Guo-Si Li · Fu-Cheng Zhu · Pei-Pei Wei ·
Fang-Li Gu · Qi-Ling Xu · Meng-Hua Ma

Received: 1 May 2022 / Accepted: 18 July 2022 / Published online: 3 August 2022
© The Author(s), under exclusive licence to Springer Nature B.V. 2022

Abstract

Objective To produce high concentrations of hyperoside from quercetin using recombinant *Escherichia coli* with in situ regeneration of UDP-galactose.

Results Sucrose synthase from *Glycine max* (GmSUS) was co-expressed with UDP-glucose epimerase from *E. coli* (GalE) in *E. coli* for regenerating UDP-galactose from UDP and sucrose. Glycosyltransferase from *Petunia hybrida* (PhUGT) was introduced to synthesize hyperoside from quercetin through the regeneration system of UDP-galactose. Co-expressing with molecular chaperones GroEL/ES successfully enhanced the catalytic efficiency of the recombinant strain, which assisted the soluble expression of PhUGT. By using a fed-batch approach, the production of hyperoside reached 863.7 mg L⁻¹ with a corresponding molar conversion of 93.6% and a specific productivity of 72.5 mg L⁻¹ h⁻¹.

Conclusion The method described herein for hyperoside production can be widely applied for the

synthesis of isorhamnetin-3-*O*-galactoside, kaempferol-3-*O*-galactoside and other flavonoids.

Keyword Glycosyltransferase · Hyperoside · Molecular chaperone · UDP-galactose regeneration · Whole cell biocatalyst

Introduction

Hyperoside (quercetin 3-*O*-galactoside) is a kind of flavonoid-*O*-glycoside, which has attracted extensive research interests due to its powerful antioxidant, cytoprotective effects (Choi et al. 2011; Piao et al. 2008) and antiviral activity against hepatitis B (Wu et al. 2007), SARS (Chen et al. 2006) viruses. Hyperoside is purified from *Zanthoxylum bungeanum* or *Hypericum perforatum* L. via solvent extraction, column chromatography, crystallization and so on (Cao et al. 2011; Fengyuan et al. 2016). However, it is a complicated process and therefore improper for mass production.

Due to environmental concerns, there is a growing interest for the biotechnological production of hyperoside (Lin et al. 2014; Putignani et al. 2013; Wang et al. 2011). The flavonol glycosyltransferase from *Petunia hybrida* (PhUGT) has been cloned and expressed in *Escherichia coli* (Miller et al. 1999), and recombinant strains harboring the PhUGT gene have been constructed to produce hyperoside (Kim et al. 2015; Li et al. 2022). However, flavonoids show

Supplementary Information The online version contains supplementary material available at <https://doi.org/10.1007/s10529-022-03285-4>.

G.-S. Li (✉) · F.-C. Zhu · P.-P. Wei · F.-L. Gu · Q.-L. Xu · M.-H. Ma

Anhui Engineering Laboratory for Conservation and Sustainable Utilization of Traditional Chinese Medicine Resources, Department of Biological and Pharmaceutical Engineering, West Anhui University, Lu'an 237012, Anhui, People's Republic of China
e-mail: liguosi1989@163.com

inhibitory effects on cell growth, influencing further improvement of the flavonoids production (De Bruyn et al. 2015b; Pei et al. 2016). These problems can be solved by enzymatic methods, but the process needs to consume UDP-galactose.

Sucrose synthase (SUS), which converts sucrose and uridine 5'-diphosphate (UDP) into UDP-glucose and fructose, has been utilized for constructing the UDP-glucose regeneration system (Gutmann et al. 2014). UDP-galactose 4-epimerase (GalE) catalyzes the interconversion between UDP-glucose and UDP-galactose (Chen et al. 1999). Sucrose synthase can be coupled with GalE to provide a simple and efficient method that can use sucrose as an inexpensive and sustainable carbon source for the synthesis of UDP-galactose.

In the present study, we described the co-expression of a SUS gene from *Glycine max* (GmSUS) and GalE from *E. coli* in *E. coli* cells for efficient in situ regeneration of UDP-galactose. Then, PhUGT was coupled with the UDP-galactose regeneration system for hyperoside production (Fig. 1). The efficiency of the recombinant strain was further improved by increasing soluble expression of PhUGT, which is a limiting step in the biocatalysis. Finally, hyperoside production using a substrate fed-batch strategy was investigated.

Material and methods

Plasmids, strains and chemicals

All plasmids and strains applied in this study were listed in Table 1. All the chemicals were purchased

Fig. 1 Construction of recombinant *Escherichia coli* for hyperoside production with in situ regeneration of UDP-galactose. UDP uridine diphosphate; GalE UDP-glucose 4-epimerase from *E. coli*; PhUGT UDP-dependent glycosyltransferases from *P. hybrida*; GmSUS Sucrose synthase from *G. max*

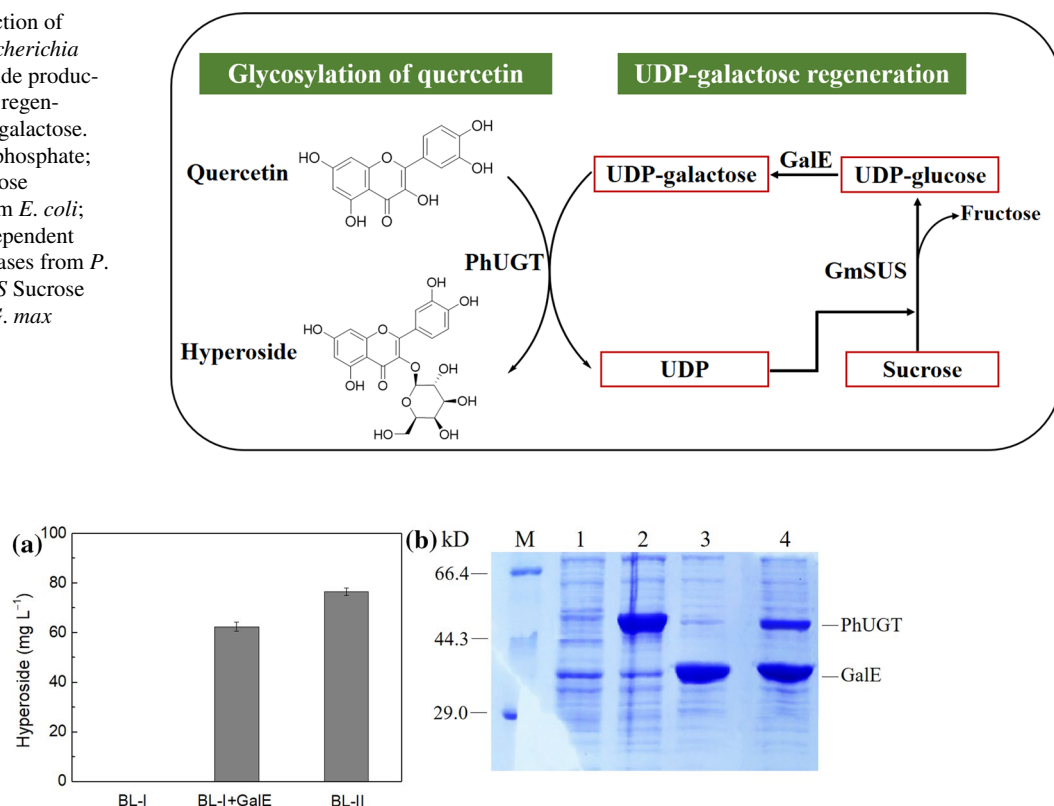


Fig. 2 Construction and performance of recombinant *E. coli*. **a** Production of Hyperoside with 151.1 mg L⁻¹ quercetin using different biocatalysts. BL-I, recombinant BL21(DE3) with pET28a-PhUGT; BL-I+GalE, BL-I with exogenous addition

of 10 mU mL⁻¹ GalE; BL-II, recombinant BL21(DE3) with pETDuet-PhUGT-GalE. **b** SDS-PAGE analysis of protein expression of various recombinant strains. M, Marker; Lane 1, BL21(DE3); Lane 2, BL-I; Lane 3, BL-GalE; Lane 4, BL-II

from Macklin (Shanghai, China) or Sangon Biotech (Shanghai, China). All chemicals were analytical or HPLC grade.

Construction of plasmids and strains

GmSUS from *G. max* (Accession No. NM_001250596.2) and PhUGT from *P. hybrida* (Accession No. AF165148.1) were cloned into pET28a between *Hind* III and *Noc* I (Sangon Biotech, Shanghai) for getting pET28a-GmSUS as well as pET28a-PhUGT (Table 1). The primers GalE-R and GalE-F (Table S1) were used to amplify *GalE* from genome of *E. coli* MG1655. The resulting PCR products were inserted into the expression vector pET28a

between *Hind* III and *Noc* I on the basis of the standard One Step Cloning Kit (Vazyme Biotech, Nanjing) for constructing recombinant plasmid pET28a-GalE (Table 1). The primers PhUGT-mcs1-R and PhUGT-mcs1-F, GalE-mcs2-R and GalE-mcs2-F (Table S1) were applied to amplify *PhUGT* and *GalE* with pET28a-PhUGT and pET28a-GalE as templates, and the fragments were inserted into *MCS1* and *MCS2* of pETDuet-1 between *Hind* III and *Nco* I, *Xho* I and *Nde* I to obtain pACYCDuet-PhUGT-GalE. *GmSUS* and *GroEL/ES* were amplified using pET28a-GmSUS, pGro7 as templates, GmSUS-mcs1-R and GmSUS-mcs1-F, GroEL/ES-mcs2-R and GroEL/ES-mcs2-F (Table S1) as the primers, and these fragments were inserted into *MCS1* and *MCS2* of pETDuet-1

Table 1 Plasmids and strains used in the present study

Plasmids or strains	Relevant properties or genetic marker	Source
<i>Plasmids</i>		
pET28a	P _{T7lac} , f1 ori, Kan ^r	Novagen
pETDuet-1	P _{T7lac} , f1 ori, Amp ^r	Novagen
pACYCDuet-1	P _{T7lac} , P15A ori, Cm ^r	Novagen
pET28a-PhUGT	pET28a+ <i>PhUGT</i> from <i>P. hybrida</i>	This study
pET28a-PhUGT	pET28a+ <i>PhUGT</i> from <i>P. hybrida</i>	This study
pET28a-GalE	pET28a+ <i>GalE</i> from <i>E. coli</i> MG1655	This study
pET28a-GmSUS	pET28a+ <i>GmSUS</i> from <i>G. max</i>	This study
pACYCDuet-PhUGT-GalE	pETDuet-1+ <i>PhUGT</i> from <i>P. hybrida</i> + <i>GalE</i> from <i>E. coli</i> MG1655	This study
pETDuet-GmSUS-GroEL/ES	pETDuet-1+ <i>GmSUS</i> from <i>G. max</i> + <i>GroEL/ES</i> from pGro7	This study
pG-KJE8	P _{araB} , P _{Pzt-1} :: <i>groEL/ES</i> + <i>dnaK/J</i> + <i>grpE</i> , Ori (pACYC184), Cm ^r	Takara
pGro7	P _{araB} :: <i>groEL/ES</i> , Ori (pACYC184), Cm ^r	Takara
pKJE7	P _{araB} :: <i>dnaK/J</i> , Ori (pACYC184), Cm ^r	Takara
pG-Tf2	P _{Pzt-1} :: <i>groEL/ES</i> + <i>tig</i> , Ori (pACYC184), Cm ^r	Takara
pTf16	P _{araB} :: <i>tig</i> , Ori (pACYC184), Cm ^r	Takara
<i>Strains</i>		
<i>E. coli</i> MG1655	F ⁻ λ ⁻ <i>ilvG</i> - <i>rfb</i> -50 <i>rph</i> -1	Novagen
BL21 (DE3)	F ⁻ <i>ompT</i> <i>hdsSB</i> (r _B ⁻ m _B ⁻) <i>gal dcm lon</i> (DE3)	Novagen
BL-GalE	BL21 (DE3) harboring pET28a-GalE	This study
BL-GmSUS	BL21 (DE3) harboring pET28a-GmSUS	This study
BL-I	BL21 (DE3) harboring pET28a-PhUGT	This study
BL-I-pG-KJE8	BL-I harboring pG-KJE8	This study
BL-I-pGro7	BL-I harboring pGro7	This study
BL-I-pKJE7	BL-I harboring pKJE7	This study
BL-I-pTf16	BL-I harboring pTf16	This study
BL-I-pG-Tf2	BL-I harboring pG-Tf2	This study
BL-II	BL21 (DE3) harboring pACYCDuet-PhUGT-GalE	This study
BL-III	BL21 (DE3) harboring pACYCDuet-PhUGT-GalE and pETDuet-GmSUS	This study
BL-IV	BL21 (DE3) harboring pACYCDuet-PhUGT-GalE and pETDuet-GmSUS- <i>groEL/ES</i>	This study

between *Hind* III and *Nco* I, *Xho* I and *Nde* I, resulting pETDuet-GmSUS-GroEL/ES.

The recombinant strains BL-GalE and BL-GmSUS were respectively obtained when plasmids pET28a-GalE and pET28a-GmSUS were transformed into *E. coli* BL21(DE3). Plasmids pACYCDuet-PhUGT-GalE and pET28a-PhUGT were converted into *E. coli* BL21(DE3) to obtain recombinant strain BL-I and BL-II (Table 1). Plasmids pET28a-GmSUS and pETDuet-GmSUS-GroEL/ES were transformed into BL-II, respectively, to obtain BL-III and BL-IV (Table 1). Chaperone plasmids pGro7, pG-KJE8, pTf16, pG-Tf2, along with pKJE7 were transformed into BL-I, respectively to obtain BL-I-pG-KJE8, BL-I-pGro7, BL-I-pKJE7, BL-I-pTf16, and BL-I-pG-Tf2 (Table 1).

Protein production using recombinant strains

Several recombinant strains such as BL-GalE, BL-GmSUS, BL-III, BL-I, BL-IV, and BL-II were cultured on 50 ml of LB medium containing certain antibiotics under the temperature of 37 °C. 0.1 mM isopropyl-d-1-thiogalactopyranoside (IPTG) was added to induce the expression of protein at 20 °C for 24 h when the absorbance at 600 nm achieved 0.8. Recombinant strains BL-I-pG-KJE8, BL-I-pGro7, BL-I-pKJE7, BL-I-pTf16, and BL-I-pG-Tf2 were initially inoculated under the temperature of 37 °C in LB medium of 50 mL containing 34 mg mL⁻¹ chloramphenicol and 50 mg mL⁻¹ kanamycin. When OD₆₀₀ achieved 0.5, 5 ng mL⁻¹ tetracycline or 0.5 mg mL⁻¹ L-arabinose was increased. When OD₆₀₀ achieved 1.0, 0.1 mM IPTG was then added to induce PhUGT expression at 20 °C for 24 h. The cells were subsequently gathered through centrifugation at 8000 rpm under a temperature of 4 °C for fifteen minutes. The supernatants were achieved by ultra-sonication (50% amplitude, 3 s pulse and 7 s pause for 15 min) and centrifugation (10,000 rpm, 4 °C for 20 min). Cell dry weight (CDW) was calculated from the OD₆₀₀ value using a ratio of 0.33 g (CDW) L⁻¹ per OD₆₀₀.

Enzyme activity

Enzyme activity of PhUGT, GmSUS and GalE were measured as described previously (Diricks et al. 2015; Miller et al. 1999; Pei et al. 2017).

Hyperoside production by recombinant *E. coli*

Batch reactions using BL-I and BL-II were performed in a 50 mL shake flask with 10 mL working-volume, which contained quercetin of 0.5 mM, 0.81 g (CDW) L⁻¹ cells, phosphate buffer of 50 mM (pH 7.5), as well as 10 g L⁻¹ glucose. Reactions were conducted at 200 rpm under the temperature of 30 °C for 12 h.

Batch reactions using BL-III and BL-IV were performed in a 50 mL shake flask with 10 mL working-volume, which contained quercetin of 0.5 mM, 0.81 g (CDW) L⁻¹, phosphate buffer of 50 mM (pH 7.5), 0.25 mM UDP as well as 500 mM sucrose. Stock solutions of quercetin (50 mM) was made up in 100% DMSO. Reactions were conducted at 200 rpm under the temperature of 30 °C for 3 h. Substrate fed-batch was conducted under the same conditions. After depletion of quercetin added initially, 0.5 mM quercetin was fed. Samples were harvested at intervals and ten volumes of methanol were added directly to stop the reaction. The supernatant was harvested by centrifugation at 12,000×g for 10 min and analyzed using high-performance liquid chromatography (HPLC).

HPLC analysis

The specimen needed to analyze by the high-performance liquid chromatography (HPLC) (HP1100, Agilent 1100 series) with a C18 column (5 μm, 4.6×250 mm, Agilent). The experiment was analyzed under the column temperature of 30 °C at 368 nm with a flow rate of 0.6 mL min⁻¹ in 55% methanol. All the assays were conducted in triplicate.

Product purification and structural identification

The fed-batch reaction solution was harvested by centrifugation at 20,000×g for 10 min. The supernatant was applied to an AB-8 column macroporous resin (2.5×30 cm, Jianghua, China) equilibrated with distilled water, and was eluted with 20 and 50% ethanol, respectively. The elution with 50% ethanol was collected and evaporated to dryness, and the product was analyzed using ¹H-NMR and ¹³C-NMR (Bruker AVANCE IIII 400) using DMSO-*d*₆ as the solvent.

Results

Co-expression of PhUGT and GalE in *E. coli*

PhUGT from *P. hybrida* was reported to be efficient for glycosylating quercetin at the 3C-O position (Kim et al. 2015; Pei et al. 2017). In this study, *PhUGT* was cloned into pET-28a(+) and expressed in *E. coli* BL21 (DE3). However, hyperoside produced using the resulted recombinant strain BL-I could not be detected (Fig. 2a). Genome analysis suggested *GalE* is absent in BL21 (DE3). Therefore, *GalE* from *E. coli* MG1655 was expressed in BL21 (DE3) (Fig. 2b) and the cell extracts were added to the reaction system. The results showed that 62.3 mg L^{-1} hyperoside was produced, indicating the successful conversion of UDP-glucose to UDP-galactose in BL21 (DE3). To simplify the expression process, *GalE* was co-expressed with *PhUGT* using pACYCDuet-1 (Fig. 2b). After 12 h of reaction, the production of hyperoside using the resulted strain BL-II reached 76.5 mg L^{-1} with a molar conversion rate of 26.8%. Thus, the recombinant strain BL-II is potential to be used in the production of hyperoside.

Construction of UDP-galactose regeneration system

UDP-sugar is a key factor in glycosylation (De Bruyn et al. 2015a, 2015b; Miller et al. 1999). Increasing the supply of UDP-galactose in the recombinant strains

is essential to improve hyperoside production. UDP-galactose is produced from UDP-glucose via *GalE* in BL21-II and thus the supply of UDP-glucose must be increased. Two methods have been reported to enhance the synthesis of UDP-glucose in *E. coli*. One is the overexpression of two key enzymes (phosphoglucomutase, Pgm, and UDP-glucose pyrophosphorylase, GalU) in *E. coli* (Yao et al. 2006) and the other is the reconstruction of a novel UDP-glucose synthesis pathway via simultaneous expression of Basp (a sucrose phosphorylase from *Bifidobacterium adolescentis*) and UgpA (a uridylyltransferase from *Bifidobacterium bifidum*) (De Bruyn et al. 2015b). However, both methods require fine regulations of gene expression and long-time transformation.

Sucrose synthase has been utilized to construct the regeneration of UDP-glucose (Gutmann et al. 2014). When GmSUS was coupled in the reaction, we could even use sucrose and UDP instead of UDP-glucose as starting materials to produce glucosides. In this research, to improve the supply of UDP-galactose, GmSUS was overexpressed in BL-II by pET28a. According to SDS-PAGE analysis, PhUGT, *GalE*, and GmSUS were successfully expressed in the resulted strain BL-III containing pET28a-GmSUS and pACYCDuet-PhUGT-GalE (Fig. 3a). Hyperoside production using the BL-III reached 172.3 mg L^{-1} , which was 2.3 times higher than that produced in BL-II (Fig. 3b). These results indicated that by introducing an UDP-galactose regeneration system, BL-III

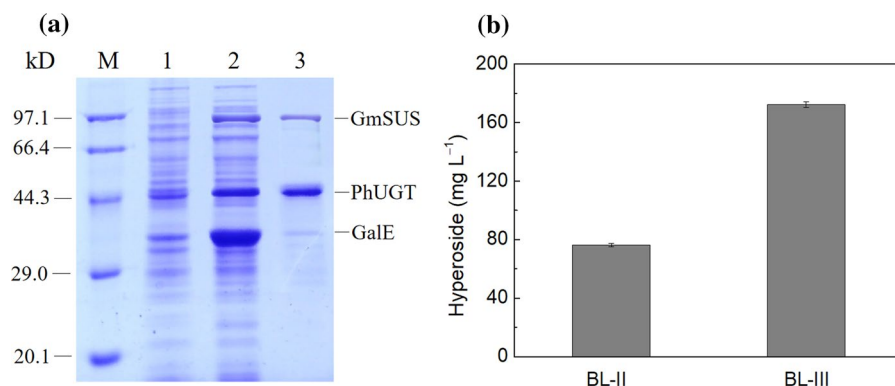


Fig. 3 Construction and performance of UDP-galactose regeneration system. **a** SDS-PAGE analysis of protein expression in BL-III harboring both pACYCDuet-PhUGT-GalE and pET-Duet-GmSUS. M, Marker; Lane 2, supernatant of BL-III; Lane

3, precipitates of BL-III; Lane 1, *E. coli* BL21(DE3); **b** Hyperoside production with 151.1 mg L^{-1} quercetin using BL-II and BL-III as whole cell biocatalysts

is able to offer more UDP-galactose for hyperoside synthesis.

Screening appropriate molecular chaperones to improve PhUGT expression

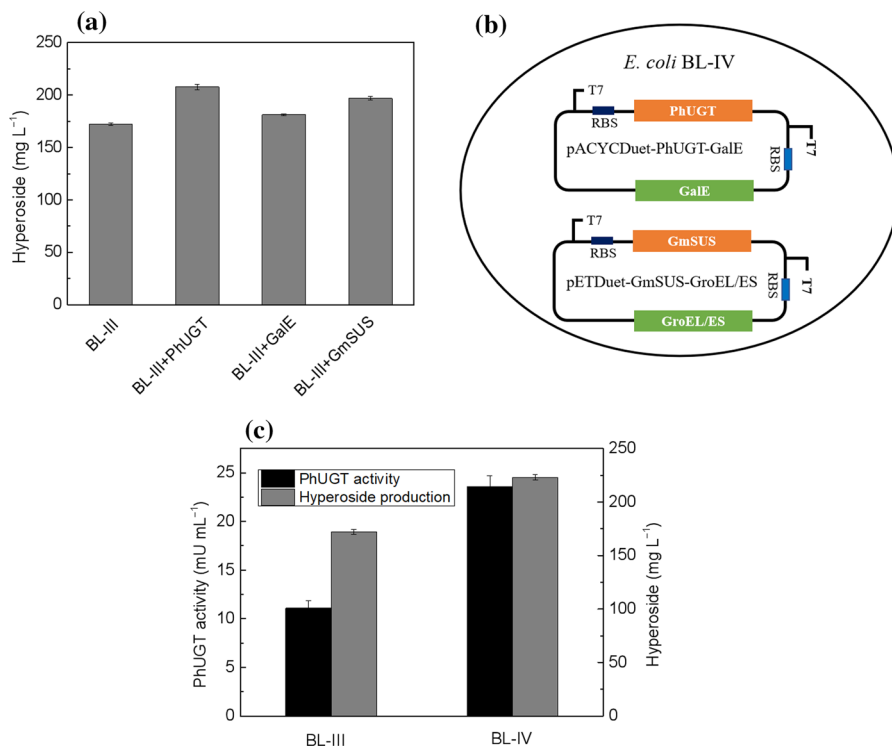
Although recombinant strain BL-III was constructed via the introduction of UDP-galactose regeneration system, hyperoside production was still low. Exogenous addition of crude extracts of 50 mU mL⁻¹ PhUGT, GalE and GmSUS to the reaction system showed that the inadequate activity of PhUGT was the bottleneck (Fig. 4a). Analysis of SDS-PAGE indicated that about half of the PhUGT was expressed in the form of inclusion bodies (Fig. 3a). Thus, it is necessary to reduce PhUGT inclusion bodies. Reportedly, co-expression of molecular chaperones can enhance soluble expression of different recombinant proteins in *E. coli* (Ashraf et al. 2017; Zhang et al. 2017). In this research, five chaperone plasmids pG-Tf2, pTf16, pKJE7, pGro7 and pG-KJE8 were transformed into BL-I. SDS-PAGE analysis of the supernatant of cell extracts showed both PhUGT and molecular chaperones were successfully expressed (Fig. S1). Compared with the recombinant *E. coli*

BL21 strain without a chaperone plasmid, the soluble PhUGT co-expressed with pGro7 was significantly increased (Fig. S1), indicating that molecular chaperones GroEL/ES improved the soluble expression of PhUGT. *GroEL/ES* was then co-expressed with *PhUGT* using pETDuet-1. The resulted plasmid pETDuet-GmSUS-GroEL/ES was transformed into BL-II to obtained recombinant strain BL-IV (Fig. 4b). As expected, PhUGT activity was significantly increased from 11.1 to 23.6 mU mL⁻¹ (Fig. 4c), indicating the successful introduction of GroEL/ES. Finally, hyperoside production using BL-IV as biocatalyst reached 222.9 mg L⁻¹ with a corresponding molar conversion of 96.0% (Fig. 4c).

Fed-batch reaction for hyperoside production

To improve the final concentration of hyperoside and prevent the inhibition of a high concentration of quercetin on activity of GmSUS (Pei et al. 2017), we added 0.5 mM fresh quercetin to the reaction mixture every time once the substrate was consumed. As shown in Fig. 5, a kinetic analysis of hyperoside production along with quercetin consumption over time was investigated. The specific productivity

Fig. 4 Enhancing hyperoside production by improving soluble expression of PhUGT. **a** Production of hyperoside by BL-III with exogenous addition of crude extracts of PhUGT, GalE and GmSUS. **b** Construction of recombinant strain BL-IV harboring pACYCDuet-PhUGT-GalE and pETDuet-GmSUS-GroEL/ES. **c** PhUGT activity after introduction and hyperoside production using BL-III and BL-IV as whole cell biocatalysts



was $102.3 \text{ mg L}^{-1} \text{ h}^{-1}$ during the first batch period. The specific productivity gradually decreased as the reaction proceeded with $98.7 \text{ mg L}^{-1} \text{ h}^{-1}$ during the second batch, $80.4 \text{ mg L}^{-1} \text{ h}^{-1}$ during the third batch, and $56.7 \text{ mg L}^{-1} \text{ h}^{-1}$ during the fourth batch. Product inhibition may be the major reason of the decrease in the specific productivity. Finally, 869.4 mg L^{-1} hyperoside was produced with the corresponding molar conversion of 93.6% and a specific productivity of $72.5 \text{ mg L}^{-1} \text{ h}^{-1}$.

Structural identification of hyperoside

^1H NMR (400 MHz, $\text{DMSO-}d_6$): 12.58 (s, 1H), 10.82 (s, 1H), 9.69 (s, 1H), 9.11 (s, 1H), 7.62 (dd, $J=1.8, 8.4 \text{ Hz}$, 1H, H-6'), 7.47 (d, $J=1.8 \text{ Hz}$, 1H, H-2'), 6.76 (d, $J=8.4 \text{ Hz}$, 1H, H-5'), 6.35 (d, $J=1.6 \text{ Hz}$, 1H, H-8), 6.15 (d, $J=1.6 \text{ Hz}$, 1H, H-6), 5.33 (d, $J=7.6 \text{ Hz}$, 1H, H-1''), 3.20–5.10 (11H) (Fig. S2). ^{13}C NMR (100 MHz, $\text{DMSO-}d_6$): 178.0 (C-4), 164.6 (C-7), 161.7 (C-5), 156.8 (C-2), 156.7 (C-9), 148.9 (C-4'), 145.3 (C-3'), 134.0 (C-3), 122.5 (C-6'), 121.6 (C-1'), 116.4 (C-5'), 115.6 (C-2'), 104.4 (C-10), 102.3 (C-1''), 99.1 (C-6), 94.0 (C-8), 76.3 (C-5''), 73.7 (C-3''), 71.7 (C-2''), 68.4 (C-4''), 60.6 (C-6'') (Fig. S3).

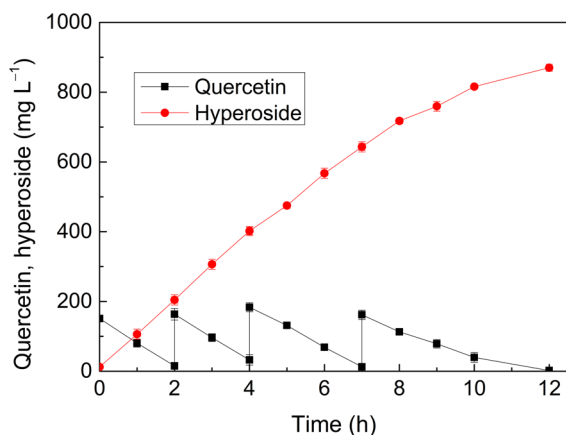


Fig. 5 Hyperoside production using recombinant strain BL-IV involving feeding of quercetin

Conclusion

In this study, a recombinant *E. coli* co-expressing PhUGT and GalE was first constructed for hyperoside production (62.3 mg L^{-1}). When additional enzyme GmSUS was introduced, the regenerative UDP-galactose catalyzed by GmSUS coupled with GalE increased hyperoside production to 172.3 mg L^{-1} . By introducing molecular chaperone GroES/EL, the soluble expression of PhUGT was successfully improved and hyperoside production reached 222.9 mg L^{-1} . By using a substrate fed-batch strategy, hyperoside production reached 869.4 mg L^{-1} with a conversion rate of 93.6% and a specific productivity of $72.5 \text{ mg L}^{-1} \text{ h}^{-1}$. In general, enzymatic glycosylation is one of the most promising methods for producing glycosides. Nevertheless, the method is restricted by the high-cost UDP-sugar. Multienzyme cascade reactions have been established for the regeneration of UDP-galactose as well as the synthesis of glycosides (Pei et al. 2017; Tsai et al. 2013). To date, the highest hyperoside production reached 2134 mg L^{-1} through the in vitro regeneration of UDP-galactose. However, the process requires the addition of various crude enzyme extracts, which is complex and time-consuming. The whole cell biocatalyst constructed herein for hyperoside production stands out because of its simplicity.

Acknowledgements This research was funded by High-level talent project of West Anhui University (WGKQ2021025) and Natural Science Foundation of Anhui Province (2008085QB96).

Supplementary Information Supplementary Table 1 Primers used in the present study.

Supplementary Fig. 1 Expression of PhUGT in *E. coli* BL21(DE3) assisted by different chaperones.

Supplementary Fig. 2 ^1H NMR spectra of purified hyperoside.

Supplementary Fig. 3 ^{13}C NMR spectra of purified hyperoside.

Funding The authors have not disclosed any funding.

Declarations

Conflict of interest The authors declare no competing financial interest.

References

- Ashraf R, Muhammad MA, Rashid N, Akhtar M (2017) Cloning and characterization of thermostable GroEL/GroES homologues from *Geobacillus thermopakistanensis* and their applications in protein folding. *J Biotech* 254:9–16
- Cao X, Wang Q, Li Y, Bai G, Ren H, Xu C, Ito Y (2011) Isolation and purification of series bioactive components from *Hypericum perforatum* L. by counter-current chromatography. *J Chromatogr B* 879:480–488
- Chen X, Kowal P, Hamad S, Fan HN, Wang PG (1999) Cloning, expression and characterization of a UDP-galactose 4-epimerase from *Escherichia coli*. *Biotech Lett* 21:1131–1135
- Chen L, Li J, Luo C, Liu H, Xu W, Chen G, Liew OW, Zhu W, Puah CM, Shen X, Jiang H (2006) Binding interaction of quercetin-3-beta-galactoside and its synthetic derivatives with SARS-CoV 3CL(pro): structure-activity relationship studies reveal salient pharmacophore features. *Bioorgan Med Chem* 14:8295–8306
- Choi J-H, Kim D-W, Yun N, Choi J-S, Isam N, Kim Y-S, Lee S-M (2011) Protective effects of hyperoside against carbon tetrachloride-induced liver damage in mice. *J Nat Prod* 74:1055–1060
- De Bruyn F, De Paep B, Maertens J, Beauprez J, De Cocker P, Mincke S, Stevens C, De Mey M (2015a) Development of an in vivo glucosylation platform by coupling production to growth: production of phenolic glucosides by a glycosyltransferase of *Vitis vinifera*. *Biotech Bioeng* 112:1594–1603
- De Bruyn F, Van Brempt M, Maertens J, Van Bellegem W, Duchi D, De Mey M (2015b) Metabolic engineering of *Escherichia coli* into a versatile glycosylation platform: production of bio-active quercetin glycosides. *Microb Cell Fact* 14:138–149
- Diricks M, De Bruyn F, Van Daele P, Walmagh M, Desmet T (2015) Identification of sucrose synthase in nonphotosynthetic bacteria and characterization of the recombinant enzymes. *App Microbi Biotech* 99:8465–8474
- Fengyuan H, Dengwu L, Dongmei W, Ming D (2016) Extraction and purification of quercitrin, hyperoside, rutin, and afzelin from *Zanthoxylum bungeanum* Maxim leaves using an aqueous two-phase system. *J Food Sci* 81:C1593–C1602
- Gutmann A, Bungaruang L, Weber H, Leypold M, Breinbauer R, Nidetzky B (2014) Towards the synthesis of glycosylated dihydrochalcone natural products using glycosyltransferase-catalysed cascade reactions. *Green Chem* 16:4417–4425
- Kim SY, Lee HR, Park K-s, Kim B-G, Ahn J-H (2015) Metabolic engineering of *Escherichia coli* for the biosynthesis of flavonoid-O-glucuronides and flavonoid-O-galactoside. *Appl Microb Biotech* 99:2233–2242
- Li G, Zhu F, Wei P, Xue H, Chen N, Lu B, Deng H, Chen C, Yin X (2022) Metabolic engineering of *Escherichia coli* for hyperoside biosynthesis. *Microorganisms* 10:628–639
- Lin YH, Jain R, Yan YJ (2014) Microbial production of anti-oxidant food ingredients via metabolic engineering. *Curr Opin Biotech* 26:71–78
- Miller KD, Guyon V, Evans JNS, Shuttleworth WA, Taylor LP (1999) Purification, cloning, and heterologous expression of a catalytically efficient flavonol 3-O-galactosyltransferase expressed in the male gametophyte of *Petunia hybrida*. *J Biol Chem* 274:34011–34019
- Pei J, Dong P, Wu T, Zhao L, Fang X, Cao F, Tang F, Yue Y (2016) Metabolic engineering of *Escherichia coli* for astragaloside biosynthesis. *J Agr Food Chem* 64:7966–7972
- Pei J, Chen A, Zhao L, Cao F, Ding G, Xiao W (2017) One-pot synthesis of hyperoside by a three-enzyme cascade using a UDP-galactose regeneration system. *J Agr Food Chem* 65:6042–6048
- Piao MJ, Kang KA, Zhang R, Ko DO, Wang ZH, You HJ, Kim HS, Kim JS, Kang SS, Hyun JW (2008) Hyperoside prevents oxidative damage induced by hydrogen peroxide in lung fibroblast cells via an antioxidant effect. *BBA-Gen Subjects* 1780:1448–1457
- Putignani L, Massa O, Alisi A (2013) Engineered *Escherichia coli* as new source of flavonoids and terpenoids. *Food Res Int* 54:1084–1095
- Tsai T-I, Lee H-Y, Chang S-H, Wang C-H, Tu Y-C, Lin Y-C, Hwang D-R, Wu C-Y, Wong C-H (2013) Effective sugar nucleotide regeneration for the large-scale enzymatic synthesis of globo H and SSEA4. *J Am Chem Soc* 135:14831–14839
- Wang YC, Chen S, Yu O (2011) Metabolic engineering of flavonoids in plants and microorganisms. *App Microb and Biotech* 91:949–956
- Wu L-l, Yang X-b, Huang Z-m, Liu H-z, Wu G-x (2007) In vivo and in vitro antiviral activity of hyperoside extracted from *Abelmoschus manihot* (L) medik. *Acta Pharmacol Sin* 28:404–409
- Yao QJ, Song J, Xia CF, Zhang WP, Wang PG (2006) Chemoenzymatic syntheses of iGb3 and Gb3. *Org Lett* 8:911–914
- Zhang Y, Qiao X, Yu X, Chen J, Hou L, Bi Z, Zheng Q, Hou J (2017) Enhanced soluble production of cholera toxin B subunit in *Escherichia coli* by co-expression of SKP chaperones. *Protein Expres Purif* 138:1–6

Publisher's Note Springer Nature remains neutral with regard to jurisdictional claims in published maps and institutional affiliations.

Springer Nature or its licensor holds exclusive rights to this article under a publishing agreement with the author(s) or other rightsholder(s); author self-archiving of the accepted manuscript version of this article is solely governed by the terms of such publishing agreement and applicable law.